Published in final edited form as:
J Cereb Blood Flow Metab. 2009 January ; 29(1): 176–185. doi:10.1038/jcbfm.2008.109.

Hemodynamic Changes Following Visual Stimulation and Breath-holding Provide Evidence for an Uncoupling of Cerebral Blood Flow and Volume from Oxygen Metabolism

Manus J. Donahue, Ph.D[1,2,3], **Robert D. Stevens, M.D**[4], **Michiel de Boorder, M.D**[5], **James J. Pekar, Ph.D**[1,2], **Jeroen Hendrikse, M.D., Ph.D**[5], and **Peter C.M. van Zijl, Ph.D.**[1,2]

[1] The Russell H. Morgan Department of Radiology and Radiological Science, Division of MR Research, The Johns Hopkins University School of Medicine, Baltimore, MD USA [2] F.M. Kirby Center for Functional Brain Imaging, Kennedy Krieger Institute, Baltimore, MD USA [3] Oxford Centre for Functional MRI of the Brain, Department of Clinical Neurology, The University of Oxford, Oxford, UK [4] Departments of Anesthesiology Critical Care Medicine, Neurology and Neurosurgery, The Johns Hopkins University School of Medicine, Baltimore, MD USA [5] Department of Radiology, University Medical Center Utrecht, Utrecht, The Netherlands

Abstract

Functional neuroimaging is most commonly performed using the blood-oxygenation-level-depend (BOLD) approach, which is sensitive to changes in cerebral blood flow (CBF), cerebral blood volume (CBV), and the cerebral metabolic rate of oxygen ($CMRO_2$). However, the precise mechanism by which neuronal activity elicits a hemodynamic response remains controversial. Here, separate visual stimulation (14s flashing checkerboard) and breath-hold (4s exhale + 14s breath-hold) experiments were performed in parallel on healthy volunteers using BOLD, CBV-weighted (CBVw) and CBF-weighted (CBFw) fMRI. Following visual stimulation, the BOLD signal persisted for 33±5s (n=9) and was bi-phasic with a negative component (undershoot), whereas CBV and CBF returned to baseline without an undershoot at 20±5s and 20±3s, respectively. Following breath-hold, the BOLD signal returned to baseline (23±7s) at the same time ($p>0.05$) as CBV (21±6s) and CBF (18±3s), without a post-stimulus undershoot. These data indicate that following visual activation, the BOLD undershoot is likely due to continued elevated $CMRO_2$. Furthermore, persisting elevated $CMRO_2$ is found when CBF and CBV have returned to baseline levels, providing evidence for an uncoupling of CBV and CBF responses from $CMRO_2$ changes. Persisting elevated $CMRO_2$ following elevated neuronal activity may be necessary to reverse neurotransmitter movements arising from excitatory postsynaptic currents.

Keywords

BOLD; brain function; CBF; CBV; neuro-vascular coupling; oxygen metabolism

Corresponding Author: Peter C.M. van Zijl, Johns Hopkins University School of Medicine, Dept. of Radiology, 217 Traylor Bldg, 720 Rutland Ave, Baltimore, MD, 21205, pvanzijl@mri.jhu.edu, Tel: 443-923-9511, Fax: 410-614-1948.

Disclosure/Conflict of Interest

The National Center for Research Resources (NCRR) is a component of the National Institutes of Health (NIH). The contents of the paper are solely the responsibility of the authors and do not necessarily represent the official view of NCRR or NIH. Dr. van Zijl is a paid lecturer for Philips Medical Systems. This arrangement has been approved by Johns Hopkins University in accordance with its conflict of interest policies.

Introduction

Functional magnetic resonance imaging (fMRI) using the blood-oxygenation-level-dependent (BOLD) technique (Ogawa *et al* 1990) has emerged as a leading research tool for detecting brain activity. BOLD contrast is derived from magnetic susceptibility changes consequential to alterations in the blood oxygenation level and therefore provides an indirect reflection of neuronal activity. Such oxygenation changes arise from the hemodynamic response to neuronal activity, which consists of ensemble changes in cerebral blood flow (CBF), cerebral blood volume (CBV) and the cerebral metabolic rate of oxygen ($CMRO_2$) (Buxton *et al* 1998; Leenders *et al* 1990; Ogawa *et al* 1993; van Zijl *et al* 1998). Despite a significant body of experimental data, the relationship between neuronal activity and the hemodynamic response is not well characterized (Buxton *et al* 2004; Frahm *et al* 2008; Hillman *et al* 2007; Lu *et al* 2004; Mandeville *et al* 1999; Yacoub *et al* 2006).

Two general pathways have been proposed to describe this relationship between neuronal activity and the hemodynamic response. In the *metabolic pathway*, hemodynamic changes are induced by vasodilatory metabolites (CO_2 and H^+) released during increased aerobic metabolism; changes in CBF and CBV are thus a direct reflection of local tissue energy demands and are coupled to changes in $CMRO_2$. Alternatively, the *neurotransmitter pathway* proposes that molecules released at the synapse during neuronal activity, such as glutamate, trigger the release of vasodilatory mediators (e.g., nitric oxide), which then increase CBF and CBV (Attwell and Iadecola 2002); according to this view, changes in CBF and CBV are not directly coupled to changes in $CMRO_2$.

Efforts to understand which of these pathways provides the best account of hemodynamic responses to brain activation have proven difficult. An important reason for this is because changes in neuronal activity, oxygen metabolism, neurotransmitter release and CBF are often in the same direction and proportional. One approach is to compare the time-dependent changes in CBF, CBV and $CMRO_2$ induced during and following cortical activation. The typical BOLD fMRI time course consists of an increase in signal intensity corresponding to increases in capillary and venous blood oxygenation, followed by a decrease in MR signal to sub-baseline intensity. The origin of this phase of reduced oxygenation, referred to as the post-stimulus undershoot, is still under discussion. Initially, it was hypothesized that the undershoot results from continued oxygen metabolism in the absence of changes in CBF (Frahm *et al* 1996). Subsequent experiments on anaesthetized mammals (Mandeville *et al* 1998; Mandeville *et al* 1999) suggested that the BOLD undershoot could be due to continued elevated venular CBV, described by the so-called delayed venular/venous compliance model (Buxton *et al* 1998). However, more recent human studies demonstrate an uncoupling of CBV, CBF and BOLD responses during the undershoot period (Frahm *et al* 2008; Lu *et al* 2004; Tuunanen *et al* 2006), which, under the assumption of negligible changes in hematocrit, point to a persisting increase in tissue oxygen metabolism. In another study, using near infrared spectroscopy in conjunction with BOLD fMRI, deoxyhemoglobin concentration remained elevated during the BOLD post-stimulus undershoot, providing more evidence for persisting tissue hypermetabolism following neuronal stimulation (Schroeter *et al* 2006). Recently, using BOLD and bolus-tracking, it was shown that the BOLD post-stimulus undershoot persisted after CBV had already returned to baseline (Frahm *et al* 2008). Collectively, these data indicate that activity-elicited changes in $CMRO_2$ can occur in the absence of changes in CBF and CBV, with the preserved coupling of responses during stimulus onset being coincidental rather than causal. Moreover, the uncoupling of metabolic and hemodynamic activity during the post-stimulus undershoot would tend to refute the metabolic account of the neurovascular relationship, and indirectly support the neurotransmitter account.

In this study, BOLD, CBV-weighted and CBF-weighted fMRI were performed using both visual stimulation and a mild hypercapnic stimulus (breath-hold), under normoxic conditions. In both of these physiological perturbations, CBV and CBF increase; however, contrary to visual activation where $CMRO_2$ increases, $CMRO_2$ is known to remain largely unchanged during a brief breath-hold (Fox and Raichle 1984; Mintun *et al* 2001; Siesjö 1978). Therefore, the comparison of breath-hold and visual stimulation may yield insight concerning the relationship of CBF, CBV and $CMRO_2$. We hypothesized that if the BOLD post-stimulus undershoot is due to a persisting oxygen metabolism, it will disappear in BOLD breath-hold experiments.

Materials and Methods

Experiment

Ten healthy participants (five female; five male) provided informed, written consent in accordance with local IRB requirements. All volunteers were placed in a supine position and scanned in a 3.0T MRI scanner (Philips Medical Systems, Best, The Netherlands). To prevent unwanted motion, the head was secured with a hook-and-loop fastener and foam padding. Heart rate, arterial oxygen saturation fraction (Y_a) and end-tidal CO_2 ($EtCO_2$) were monitored immediately before, during and after each fMRI task using an MR-compatible patient monitoring system (Invivo Research Inc., Orlando, FL, USA). Blood pressure and temperature (Braun, ThermoScan Pro 3000, Kronberg, Germany) were recorded before the first experiment began and after the conclusion of the final experiment.

Two BOLD, CBV-weighted (CBVw), and CBF-weighted (CBFw) scans were performed for each participant in a single slice centered on the visual cortex. The readout technique and spatial resolution were identical in all scans, namely a single-shot gradient echo echo planar imaging (EPI) sequence (SENSitivity Encoding, SENSE, factor 2.5) with FOV=240×240 mm^2 and voxel size=3×3×3 mm^3. Scan parameters for BOLD were TR/TE=3000/45 ms, 112 image acquisitions (dynamics). CBFw imaging was achieved with the transfer-insensitive labeling technique for arterial spin labeling, TILT-ASL (Golay *et al* 1999): FOV=240×240 mm^2, voxel size=3×3×3 mm^3, single-shot gradient echo EPI, TR/TI/TE=2000/1500/13 ms, 168 combined control and label image acquisitions. TILT-ASL scan parameters were optimized for specific CBF sensitivity (Donahue *et al* 2006b). CBVw imaging was achieved with the vascular space occupancy (VASO) approach (Lu *et al* 2003): TR/TI/TE=5000/1054/13 ms and 68 image acquisitions. The TR and TE values for the two methods were chosen to optimize the desired contrast for each technique. For instance, for BOLD fMRI a TR of 3000 ms was used to avoid inflow effects and the interference of stimulated echoes, while a TR of 5000 ms was needed for VASO to optimize for CBV sensitivity (Donahue *et al* 2006a), which was not done in earlier work when the VASO contrast mechanism was less well understood. The TR discrepancy (ASL TR=2000 ms, VASO TR=5000 ms and BOLD TR=3000 ms) should be kept in mind when interpreting results, and time course differences that are less than 3000 ms may be insignificant. The CBVw signal change is fundamentally negative owing to the nature of the VASO contrast mechanism (Lu *et al* 2003), however the time courses have been inverted here to make direct comparison with BOLD and CBFw time courses more straightforward.

Recent work has shown that, in addition to CBV, the VASO contrast is sensitive to other parameters, such as CBF, water exchange between compartments, blood inflow, and CSF partial volume contributions (Donahue *et al* 2006a; Scouten and Constable 2008). Fortunately, while short TR experiments are affected by all of these effects, long TR VASO is predominantly sensitive to CBV (Donahue *et al* 2006a). Early VASO experiments in humans (Donahue *et al* 2006a; Lu *et al* 2003), as well as high-resolution independent experiments in cats at high magnetic field (Jin and Kim 2006; Jin and Kim 2008) have shown that the VASO effects are well localized within the microvasculature, consistent with the presumed CBV origin.

BOLD, CBVw and CBFw hemodynamic responses were measured in each participant using two experimental paradigms. In the first, a visual task consisting of 56s cross-hair fixation followed by 14s blue/yellow flashing (frequency=8 Hz) checkerboard stimulation, was repeated four times. In the second, a breath-hold task consisting of 52s normal breathing, 4s exhalation, and 14s breath-holding, was repeated four times. Each subject had 56s of resting/normal breathing at the beginning of each scan to become accustomed to scanner noise and for magnetization to reach steady-state; data acquired during this time were not analyzed. During the initial experimental planning, longer breath-holds (20-30s) were attempted, but it was found that these were followed by mild hyperventilation, which will cause a negative BOLD response and could be erroneously interpreted as a post-stimulus undershoot. Therefore, to prevent this unwanted compensatory response, the breath-hold task was reduced to 14s, which was short enough to minimize unwanted respiratory compensation. Participants were instructed to refrain from using hemodynamic stimulants (coffee, tea, chocolate, licorice) for six hours prior to their participation, and also to arrive at least fifteen minutes prior to the start of the study to rehearse the paradigms.

Data Analysis

First, images were corrected for motion and co-registered using the Oxford Centre for Functional Magnetic Resonance Imaging of the Brain (FMRIB) Linear Image Registration Tool (FLIRT) (Jenkinson and Smith 2001). As a gradient echo single-shot EPI readout was used in all scans, distortions were comparable in BOLD, CBVw and CBFw scans. Next, images were corrected for baseline drift using a cubic-spline interpolation algorithm written in MATLAB (The MathWorks, Natick, Massachusetts).

A *z*-test was used to identify activated voxels. Voxel selection criteria for activation were *z*-score≥2.5 (BOLD, ASL), *z*-score≤−2.5 (VASO), SNR≥20 (BOLD, VASO), and cluster size≥4 (BOLD, CBVw and CBFw). A paired *t*-test was used to determine statistical significance. In CBFw TILT-ASL, BOLD artifacts were reduced by linearly interpolating consecutive *control* images, from which the interior label image was subtracted (Lu *et al* 2006). In this correction approach, three ASL images (e.g. two control and one label) are required to generate a single CBFw image. To account for the added time required to generate a single CBFw image (effectively two additional TRs), the ASL time course was shifted by 2s to reflect the center of all ASL images used for calculating the CBFw image.

Two methods were applied for activation map selection. In *Method 1*, comparison of signal changes *within imaging modalities* (e.g. BOLD, CBVw or CBFw) was designed. This was achieved by calculating time courses only in voxels meeting activation criteria in visual *and* breath-hold experiments for each imaging modality. In *Method 2*, to compare signal changes *between imaging modalities*, BOLD, CBVw, and CBFw visual *or* breath-hold activation maps were combined to yield a new activation map that described only voxels meeting activation criteria in *all* modalities, separately for each task (visual or breath-hold). Note that *Method 1* allows for comparison between tasks for each imaging modality; *Method 2* allows for comparison between imaging modalities for a single task.

Notice that it is not a good approach to use all activated BOLD voxels as a template and subsequently compute CBVw and CBFw changes in these voxels. This approach is problematic as BOLD effects also occur in draining veins, leading to inaccurate localization of activation.

Results

Ten healthy participants were scanned in this study. However, one of the participants was not able to perform all tasks and was excluded. Table 1 shows mean physiological values acquired both before and immediately after the task periods. Vital signs were not found to deviate

significantly ($p>0.01$) either between visual and breath-hold experiments or within task periods. Body temperature (begin: 36.6±0.3 °C; end: 36.8±0.3 °C) and blood pressure (begin: systolic=125.0±17.0 mmHg, diastolic=70.0±10.7 mmHg; end: systolic=114.6±14.2 mmHg, diastolic=69.8±10.5 mmHg) varied insignificantly ($p>0.01$) from the beginning and end of the experiment. Note that $EtCO_2$ was similar before and after breath-hold periods, indicating that compensatory hyperventilation was not occurring. $EtCO_2$ recordings acquired *during* the breath-hold were zero in all subjects, which confirmed that the breath-hold was being performed.

Fig. 1 shows the averaged hemodynamic responses for the visual and breath-hold stimuli for voxels analyzed according to *Method 1*. Recall that in Method 1, comparison between visual and breath-hold stimuli can be drawn within imaging modalities, but not between imaging modalities. The data show that onset of signal changes differs between visual and breath-hold, but it is important to notice that this is not due to a physiological effect but due to the paradigm design. For visual stimulation, a 56s baseline was followed by a 14s flashing-checkerboard presentation. For breath-hold, 52s of baseline was followed by 4s for exhale and then 14s breath-hold. Therefore, while the lengths of the visual and breath-hold tasks were defined equally, the baseline period varied between tasks. It was observed that in most volunteers, BOLD, CBVw and CBFw signals already increased during the exhale period. Consequently, the actual breath-hold task was slightly longer than the visual task, with the precise length depending on how quickly volunteers exhaled. The volunteers practiced exhaling prior to scanning, however performance varied slightly. As the goal of the study was to investigate the post-stimulus events, this was not an overwhelming complication.

The data in Fig. 1 show two clear trends. First, the BOLD signal change between baseline and visual stimulation (3.4±0.8%) is larger than between baseline and breath-hold (2.3±0.3%), while the opposite effect is found in the CBVw scans (3.8±1.1% versus 5.6±1.0%, respectively). In the CBFw experiments, the signal changes did not differ significantly ($p>0.01$) between visual (67±10%) and breath-hold (60±12%) tasks. Second, a post-stimulus undershoot is present in the BOLD response to visual stimulation, while no undershoot is apparent in the BOLD response following breath-hold (Figs. 1a,b). Although the BOLD visual response crosses the baseline quickly following cessation of stimulation, the ultimate return of the BOLD signal to baseline is delayed due to the undershoot. In the CBVw and CBFw response, no undershoot is apparent (Figs. 1c-f) and both visual and breath-hold time courses return to baseline at approximately the same time.

The BOLD, CBVw and CBFw hemodynamic responses for visual and breath-hold stimuli analyzed according to Method 2 are compared in Fig. 2. The quantitative signal changes for each volunteer are shown in Table 2 and baseline return times are shown in Table 3. Recall that in the Method 2 voxel selection, comparison between BOLD, CBVw and CBFw time courses can be made for a single task (either visual or breath-hold). Following visual stimulus, the BOLD response, while crossing the baseline more rapidly, is delayed in its ultimate return to baseline (33±5s) when compared to the CBVw response (20±5s) and CBFw response (20 ±3s). This difference, due to the long post-stimulus undershoot, is highly significant ($p<0.001$). Fig. 2b shows the normalized time courses, where the maximum signal change for each imaging modality has been equated for purposes of timing comparisons. For the breath-hold experiments (Fig. 2c,d), no disparity between BOLD and CBVw or BOLD and CBFw baseline return time is apparent ($p>0.01$), owing to the absence of an undershoot.

As with the Method 1 analysis, voxels analyzed according to Method 2 (Fig. 2; Tables 2–3) yield a higher CBVw response ($p=0.01$) in breath-holding experiments (5.8±1.9%) compared to visual stimulation experiments (3.4±0.6%), whereas the CBFw response does not vary significantly between tasks ($p>0.01$). The BOLD response is reduced in breath-hold (2.2

±1.1%) compared with visual stimulation (4.2±1.2%), a finding that was found to be significant ($p<0.01$). Therefore, while the absolute signal changes vary slightly between the Method 1 and Method 2 analysis, the trends observed between task periods and imaging modalities are similar.

Discussion

The BOLD data presented here show a clear post-stimulus undershoot following visual stimulation and no undershoot following breath-hold. While the CBVw and CBFw hemodynamic responses returned to baseline at approximately the same time as the BOLD response following a breath-hold task, there was a clear discrepancy between responses following visual stimulation, where a post-stimulus BOLD undershoot occurred that continued for approximately 13s after the CBVw and CBFw responses had returned to baseline. This provides clear evidence that the BOLD signal can change in the absence of changes in CBV and CBF.

The data reported here support our hypothesis that the BOLD undershoot observed after visual stimulation is not present in breath-hold experiments if the undershoot is due to persisting increases in oxygen metabolism. Oxygen metabolism has been well-documented to remain unchanged during short breath-holds (Siesjö 1978) which is consistent with negligible changes in tissue pO_2. The changes in blood oxygenation causing a positive BOLD response during breath-hold are due to a vascular response based on a change in blood flow, under conditions of limited changes in arterial oxygenation but increased capillary and venous oxygenation. The reason is that the BOLD effect originates predominantly from changes in the concentration ratio of deoxyhemoglobin to total hemoglobin ([Hb]/[HbT]) in the capillaries, venules and veins (Ogawa *et al* 1993; van Zijl *et al* 1998). Taking into account changes in arterial oxygenation fraction ($Y_a = S_{aO2}/100$), the venous fraction of deoxyhemoglobin [Hb] relative to the total hemoglobin [HbT], is (van Zijl *et al* 1998):

$$\frac{[Hb]}{[HbT]}=1-Y_a+OEF\cdot Y_a=1-Y_a+\frac{CMRO_2}{CBF\bullet[HbT]\bullet Y_a}\cdot Y_a=1-Y_v, \quad [1]$$

in which the oxygen extraction fraction (OEF) is the ratio of the rate of cerebral oxygen metabolism ($CMRO_2$) and delivery. The oxygen delivery is the product of arterial oxygen content ($[HbT]\cdot Y_a$) and CBF. During brain activation, there is a mismatch between increases in $CMRO_2$ and CBF, leading to a decrease in [Hb]/[HbT] and a corresponding increase in venous oxygenation (Y_v), ultimately yielding an MRI signal increase. Notice that a similar expression applies to capillary BOLD effects, where capillary oxygenation fraction (Y_c) varies as a function of distance between arterioles and venules.

Equation [1] underlies both BOLD intra- and extra-vascular signal effects and shows that an increase in oxygenation reduces the deoxygenated Hb concentration, which amounts to a reduction in a paramagnetic MR contrast agent and thus an increase in MRI signal. Intra- and extra-vascular effects contribute to the total BOLD relaxation rates in an approximate 40/60 ratio at 3T (Lu and van Zijl 2005). For signal changes, this ratio depends on the echo time TE. At the echo time (TE = 45 ms) used here, it can be assumed that the BOLD signal change is predominantly of extra-vascular origin because there is limited venular and venous blood signal left at 3.0T. A convenient expression describing most of the venular extravascular BOLD signal changes has been given by (Yablonskiy and Haacke 1994):

$$R'_{2,Hb}\sim[HbT]\cdot CBV_v\cdot(1-Y_v), \quad [2a]$$

in which $R'_{2,Hb}$ is the deoxyhemoglobin contribution to the MRI relaxation rate and the subscript *v* denotes venular/venous as based on oxygenation. Combining equations [1] and [2a] under conditions of normoxia ($Y_a \approx 1$) gives:

$$R'_{2,Hb} \sim CBV_v \frac{CMRO_2}{CBF}. \quad [2b]$$

Thus, while an increase in blood flow reduces the relaxation rate, leading to a signal increase, any increase in CBV reduces the extravascular BOLD effect. Interestingly, the hematocrit-based term ([HbT]) vanishes in this extravascular term, indicating that hematocrit influences predominately intravascular BOLD effects. Equation [2b] indicates that, under normoxic conditions, the post stimulus undershoot must either be due to a continued increase in $CMRO_2$ or due to continued expansion of the postcapillary/venular space. A BOLD post-stimulus undershoot was not detected in breath-hold experiments, while a vascular compliance similar to neuronal activation would be expected. This suggests that the BOLD undershoot after visual stimulation is not due to delayed venular/venous compliance as suggested earlier (Buxton *et al* 1998). This accords with recent high-resolution optical imaging data showing that most vasodilation occurring during neuronal activation is due to arteriolar and capillary expansion (Hillman *et al* 2007), while venous vessel size does not change appreciably. In principle, delays in capillary compliance could contribute to a post-stimulus undershoot, but this would also be reflected in CBVw or CBFw changes, which are absent.

We therefore conclude that the post-stimulus undershoot is due to continued oxygen metabolism after changes in CBF and CBV have ceased. It has been suggested that the majority of energy utilized in gray matter during neuronal signaling is spent on reversing ionic balance following both the transmission of action potentials and excitatory postsynaptic currents. In humans, the large number of synapses per neuron and high fraction of mitochondria in dendrites leads to an expected large energy demand in post-synaptic neurons (Attwell and Laughlin 2001). Using knowledge of the synapse density in primates combined with data from energy budget experiments in rodents, it is believed that approximately 74% of signaling-related energy consumption in primates occurs in post-synaptic neurons (Attwell and Laughlin 2001; Attwell and Iadecola 2002). Therefore, a persisting elevated $CMRO_2$ could be required to reverse ion gradient across the cell membrane. Specifically, ATP is required to restore Na + and K+ concentrations across the cell membrane via the Na+/K+ pump as well as to reverse Ca^{2+} concentrations via the Na+/Ca^{2+} exchanger (Attwell and Iadecola 2002). Other smaller energy demanding processes consist of reversing ion gradients generated from the transmission of action potentials, maintaining neural resting potential and recycling neurotransmitters, the sum of which are expected to consume less energy than the above-mentioned post- synaptic ion shuttling, however. Finally, it should be noted that $CMRO_2$ changes in the absence of CBF and CBV changes reveal that following neuronal activation, energy consumption need not be coupled to hemodynamic changes. It is possible that this is true during neuronal activity as well, as suggested by the neurotransmitter pathway, however this cannot be claimed with certainty from the data presented here.

It is useful to consider these results in light of previous studies using contrast agents. First VASO-measured CBV changes following visual stimulation returned to baseline before the BOLD undershoot returned to baseline (20±5s for CBVw vs. 33±5s for BOLD; $p<0.01$). This is in contrast to previous results using MION both in anaesthetized rats (Mandeville *et al* 1999) and awake macaque monkeys (Leite *et al* 2002). Recent work at high-field (9.4T) in cats showed that the MION-measured CBV changes varied considerably with voxel location (Yacoub *et al* 2006). Specifically, CBV in surface vessels returned to baseline quickly following stimulation, whereas CBV response in tissue was more delayed. Therefore, the

location of the voxel combined with its composition of tissue and vasculature may influence the CBV dynamics. One possible reason for this is that exchange between water in blood and tissue occurs in parenchyma, whereas in large vessels no such exchange occurs. Also, capillary compliance effects could play a role and MION contrast depends strongly on hematocrit, the effects of which may be larger in tissue than in draining veins. Also, changes in blood oxygenation could compete with the MION-based CBV measurements in such tissue voxels, which would in turn alter the time course. Studies which show the effect of hematocrit on both MION and CBVw contrast may help solve the discrepancy between these two methods. Finally, recent work using contrast agents in humans has provided evidence for a quick return to baseline of CBV following neuronal stimulation (Frahm *et al* 2008). Therefore, the discrepancy between the earlier MION results may be due to a difference in vascular physiology between humans and animals or sedation used in some of the latter experiments.

One unexpected result of the current study was the finding of smaller BOLD breath-hold signal changes (2.3±0.3%) compared with the BOLD visual signal changes (3.4±0.8%) (Method 1). This was especially surprising in view of the lack of a significant difference in CBFw changes between the two tasks and the expectation that there is an increase in oxygen metabolism during neuronal stimulation. As shown in Eq. 2, the only explanation for such a reduced BOLD signal during breath-hold could be CBV increasing more during breath-hold than during visual stimulation, which was in fact observed in the CBVw time courses (Fig. 2c). Notice that this is not necessarily counterintuitive, since oxygenation is low in capillaries compared to tissue, and a larger CBV change would decrease the magnitude of the extravascular BOLD effect. It is plausible that CBV reactivity would increase more during breath-holding than during visual stimulation due to the larger strain breath-holding places on the vasculature. Because no significant discrepancy in CBF change between visual and breath-hold was observed, which would be expected in view of the large CBVw change and the often-used Grubb relationship (Grubb *et al* 1974) between CBV and CBF, it seems that the additional CBV change during breath hold is occurring in vasculature that may not be spatially related to CBF changes. Thus, the relationship between CBF and CBV in breath-hold may not be identical to the relationship that is generally found in visual or motor stimulation. Discrepancies in the relationship between CBV and CBF responses have even been reported for hypercapnia versus hypocapnia experiments (Fortune *et al* 1995). Therefore, when calibrating the BOLD effect, it may be necessary to perform a CBV calibration in addition to a CBF calibration.

Contrary to previous studies where the CBVw time course returned to baseline quickly (~10s) following cessation of stimulus (Lu *et al* 2004), we found that the CBV response is somewhat more delayed (~20s). A likely explanation for this new finding is the longer TR which was used in the current experiments, which sensitizes the sequence specifically to CBV. At short TR (TR≤3000 ms), CBF and inflow likely influence the CBVw time course. This delay may be in line with somewhat slow capillary compliance, similar to the tissue results by Yacoub et al (Yacoub *et al* 2006).

Finally, several limitations of the present study should be noted. First, a different scan repetition time, TR, was used for each imaging modality, which may in principle complicate comparison and interpretation of the signal changes. Specifically, the temporal resolution at which CBF, CBV and $CMRO_2$ coupling can be interpreted is limited by the TR of the longest (CBVw) scan (TR=5s). However, as the BOLD undershoot persisted for approximately 10s following return of CBFw and CBVw signal to baseline, it was possible to reliably identify the uncoupling of $CMRO_2$ from CBF and CBV. Second, as with most fMRI paradigms, there is always the possibility of variability in volunteer compliance. We attempted to minimize variations by having volunteers practice the paradigm before entering the magnet and also by monitoring respiratory rate and $EtCO_2$ during the scan. However, different volunteers will perform the task, especially the breath-hold, slightly differently. Finally, BOLD, CBVw and CBFw

reactivity were recorded for identical tasks, but not simultaneously. It is possible that volunteers could have performed different tasks differently, especially toward the end of the experiment when fatigue may have been an issue. We randomized the order of the scans in each volunteer, and therefore any compliance trend over time should not be present in the averaged data.

In conclusion, BOLD, CBVw and CBFw experiments were performed at 3.0T in humans to study the dynamics of CBV, CBF and $CMRO_2$ following both visual stimulation and breath-holding. First, it was found that the ultimate return of the BOLD signal to baseline is faster following breath-holding than following visual stimulation, where a post-stimulus negative signal change occurs. Since changes in $CMRO_2$ have been reported to be negligible during short breath-holds, the discrepancy in the visual and breath-hold post-stimulus changes was attributed to $CMRO_2$ changes. This observation is consistent with the BOLD visual post-stimulus signal being attributable to continued oxygen metabolism. Second, it was found that the BOLD post-stimulus undershoot persisted during a period where the CBVw and CBFw signal returned to baseline, suggestive of changes in $CMRO_2$ in the absence of changes in CBV and CBF. Therefore, $CMRO_2$ may become uncoupled from CBV/CBF following, and potentially during, neuronal activity. Persisting elevated $CMRO_2$ following cessation of neuronal activity is believed to be required to restore ion concentrations across the cell membrane. An additional finding comparing visual and breath-hold activation showed that even CBV and CBF can be decoupled depending on the stimulation used. Therefore, both CBF and CBV knowledge may be necessary for BOLD calibration experiments using hypercapnia.

Acknowledgments

Funding/Support: NIH-NIBIB R01-EB004130 and NIH-NCRR P41-RR15241.

We are grateful to Joe Gillen, Terri Brawner, Katheen Kahl and Ivana Kusevic for experimental and technical assistance. This publication was made possible by grant support from NIH-NIBIB R01-EB004130 and NIH-NCRR P41-RR15241.

References

Attwell D, Laughlin SB. An energy budget for signaling in the grey matter of the brain. J Cereb Blood Flow Metab 2001;21:1133–45. [PubMed: 11598490]

Attwell D, Iadecola C. The neural basis of functional brain imaging signals. Trends Neurosci 2002;25:621–5. [PubMed: 12446129]

Buxton RB, Wong EC, Frank LR. Dynamics of blood flow and oxygenation changes during brain activation: the balloon model. Magn Reson Med 1998;39:855–64. [PubMed: 9621908]

Buxton RB, Uludag K, Dubowitz DJ, Liu TT. Modeling the hemodynamic response to brain activation. Neuroimage 2004;23(Suppl 1):S220–33. [PubMed: 15501093]

Donahue MJ, Lu H, Jones CK, Edden RA, Pekar JJ, van Zijl PC. Theoretical and experimental investigation of the VASO contrast mechanism. Magn Reson Med 2006a;56:1261–73. [PubMed: 17075857]

Donahue MJ, Lu H, Jones CK, Pekar JJ, van Zijl PC. An account of the discrepancy between MRI and PET cerebral blood flow measures. A high-field MRI investigation. NMR Biomed 2006b;19:1043–54. [PubMed: 16948114]

Fortune JB, Feustel PJ, deLuna C, Graca L, Hasselbarth J, Kupinski AM. Cerebral blood flow and blood volume in response to O2 and CO2 changes in normal humans. J Trauma 1995;39:463–71. discussion 71–2. [PubMed: 7473910]

Fox PT, Raichle ME. Stimulus rate dependence of regional cerebral blood flow in human striate cortex, demonstrated by positron emission tomography. J Neurophysiol 1984;51:1109–20. [PubMed: 6610024]

Frahm J, Kruger G, Merboldt KD, Kleinschmidt A. Dynamic uncoupling and recoupling of perfusion and oxidative metabolism during focal brain activation in man. Magn Reson Med 1996;35:143–8. [PubMed: 8622575]

Frahm J, Baudewig J, Kallenberg K, Kastrup A, Merboldt KD, Dechent P. The post-stimulation undershoot in BOLD fMRI of human brain is not caused by elevated cerebral blood volume. Neuroimage 2008;40:473–81. [PubMed: 18201912]

Golay X, Stuber M, Pruessmann KP, Meier D, Boesiger P. Transfer insensitive labeling technique (TILT): application to multislice functional perfusion imaging. J Magn Reson Imaging 1999;9:454–61. [PubMed: 10194717]

Grubb RL Jr, Raichle ME, Eichling JO, Ter-Pogossian MM. The effects of changes in PaCO2 on cerebral blood volume, blood flow, and vascular mean transit time. Stroke 1974;5:630–9. [PubMed: 4472361]

Hillman EM, Devor A, Bouchard MB, Dunn AK, Krauss GW, Skoch J, Bacskai BJ, Dale AM, Boas DA. Depth-resolved optical imaging and microscopy of vascular compartment dynamics during somatosensory stimulation. Neuroimage 2007;35:89–104. [PubMed: 17222567]

Jenkinson M, Smith S. A global optimisation method for robust affine registration of brain images. Med Image Anal 2001;5:143–56. [PubMed: 11516708]

Jin T, Kim SG. Spatial dependence of CBV-fMRI: a comparison between VASO and contrast agent based methods. Conf Proc IEEE Eng Med Biol Soc 2006;1:25–8. [PubMed: 17946773]

Jin T, Kim SG. Improved cortical-layer specificity of vascular space occupancy fMRI with slab inversion relative to spin-echo BOLD at 9.4 T. Neuroimage 2008;40:59–67. [PubMed: 18249010]

Leenders KL, Perani D, Lammertsma AA, Heather JD, Buckingham P, Healy MJ, Gibbs JM, Wise RJ, Hatazawa J, Herold S, et al. Cerebral blood flow, blood volume and oxygen utilization. Normal values and effect of age. Brain 1990;113 (Pt 1):27–47. [PubMed: 2302536]

Leite FP, Tsao D, Vanduffel W, Fize D, Sasaki Y, Wald LL, Dale AM, Kwong KK, Orban GA, Rosen BR, Tootell RB, Mandeville JB. Repeated fMRI using iron oxide contrast agent in awake, behaving macaques at 3 Tesla. Neuroimage 2002;16:283–94. [PubMed: 12030817]

Lu H, Golay X, Pekar JJ, Van Zijl PC. Functional magnetic resonance imaging based on changes in vascular space occupancy. Magn Reson Med 2003;50:263–74. [PubMed: 12876702]

Lu H, Golay X, Pekar JJ, Van Zijl PC. Sustained poststimulus elevation in cerebral oxygen utilization after vascular recovery. J Cereb Blood Flow Metab 2004;24:764–70. [PubMed: 15241184]

Lu H, van Zijl PC. Experimental measurement of extravascular parenchymal BOLD effects and tissue oxygen extraction fractions using multi-echo VASO fMRI at 1.5 and 3.0 T. Magn Reson Med 2005;53:808–16. [PubMed: 15799063]

Lu H, Donahue MJ, van Zijl PC. Detrimental effects of BOLD signal in arterial spin labeling fMRI at high field strength. Magn Reson Med 2006;56:546–52. [PubMed: 16894581]

Mandeville JB, Marota JJ, Kosofsky BE, Keltner JR, Weissleder R, Rosen BR, Weisskoff RM. Dynamic functional imaging of relative cerebral blood volume during rat forepaw stimulation. Magn Reson Med 1998;39:615–24. [PubMed: 9543424]

Mandeville JB, Marota JJ, Ayata C, Zaharchuk G, Moskowitz MA, Rosen BR, Weisskoff RM. Evidence of a cerebrovascular postarteriole windkessel with delayed compliance. J Cereb Blood Flow Metab 1999;19:679–89. [PubMed: 10366199]

Mintun MA, Lundstrom BN, Snyder AZ, Vlassenko AG, Shulman GL, Raichle ME. Blood flow and oxygen delivery to human brain during functional activity: theoretical modeling and experimental data. Proc Natl Acad Sci U S A 2001;98:6859–64. [PubMed: 11381119]

Ogawa S, Lee TM, Kay AR, Tank DW. Brain magnetic resonance imaging with contrast dependent on blood oxygenation. Proc Natl Acad Sci U S A 1990;87:9868–72. [PubMed: 2124706]

Ogawa S, Menon RS, Tank DW, Kim SG, Merkle H, Ellermann JM, Ugurbil K. Functional brain mapping by blood oxygenation level-dependent contrast magnetic resonance imaging. A comparison of signal characteristics with a biophysical model. Biophys J 1993;64:803–12. [PubMed: 8386018]

Schroeter ML, Kupka T, Mildner T, Uludag K, von Cramon DY. Investigating the post-stimulus undershoot of the BOLD signal--a simultaneous fMRI and fNIRS study. Neuroimage 2006;30:349–58. [PubMed: 16257236]

Scouten A, Constable RT. VASO-based calculations of CBV change: accounting for the dynamic CSF volume. Magn Reson Med 2008;59:308–15. [PubMed: 18228581]

Siesjö, BK. Brain energy metabolism. Vol. xii. Chichester, [Eng.] ; New York: Wiley; 1978. p. 607

Tuunanen PI, Vidyasagar R, Kauppinen RA. Effects of mild hypoxic hypoxia on poststimulus undershoot of blood-oxygenation-level-dependent fMRI signal in the human visual cortex. Magn Reson Imaging 2006;24:993–9. [PubMed: 16997068]

van Zijl PC, Eleff SM, Ulatowski JA, Oja JM, Ulug AM, Traystman RJ, Kauppinen RA. Quantitative assessment of blood flow, blood volume and blood oxygenation effects in functional magnetic resonance imaging. Nat Med 1998;4:159–67. [PubMed: 9461188]

Yablonskiy DA, Haacke EM. Theory of NMR signal behavior in magnetically inhomogeneous tissues: the static dephasing regime. Magn Reson Med 1994;32:749–63. [PubMed: 7869897]

Yacoub E, Ugurbil K, Harel N. The spatial dependence of the poststimulus undershoot as revealed by high-resolution BOLD- and CBV-weighted fMRI. J Cereb Blood Flow Metab 2006;26:634–44. [PubMed: 16222242]

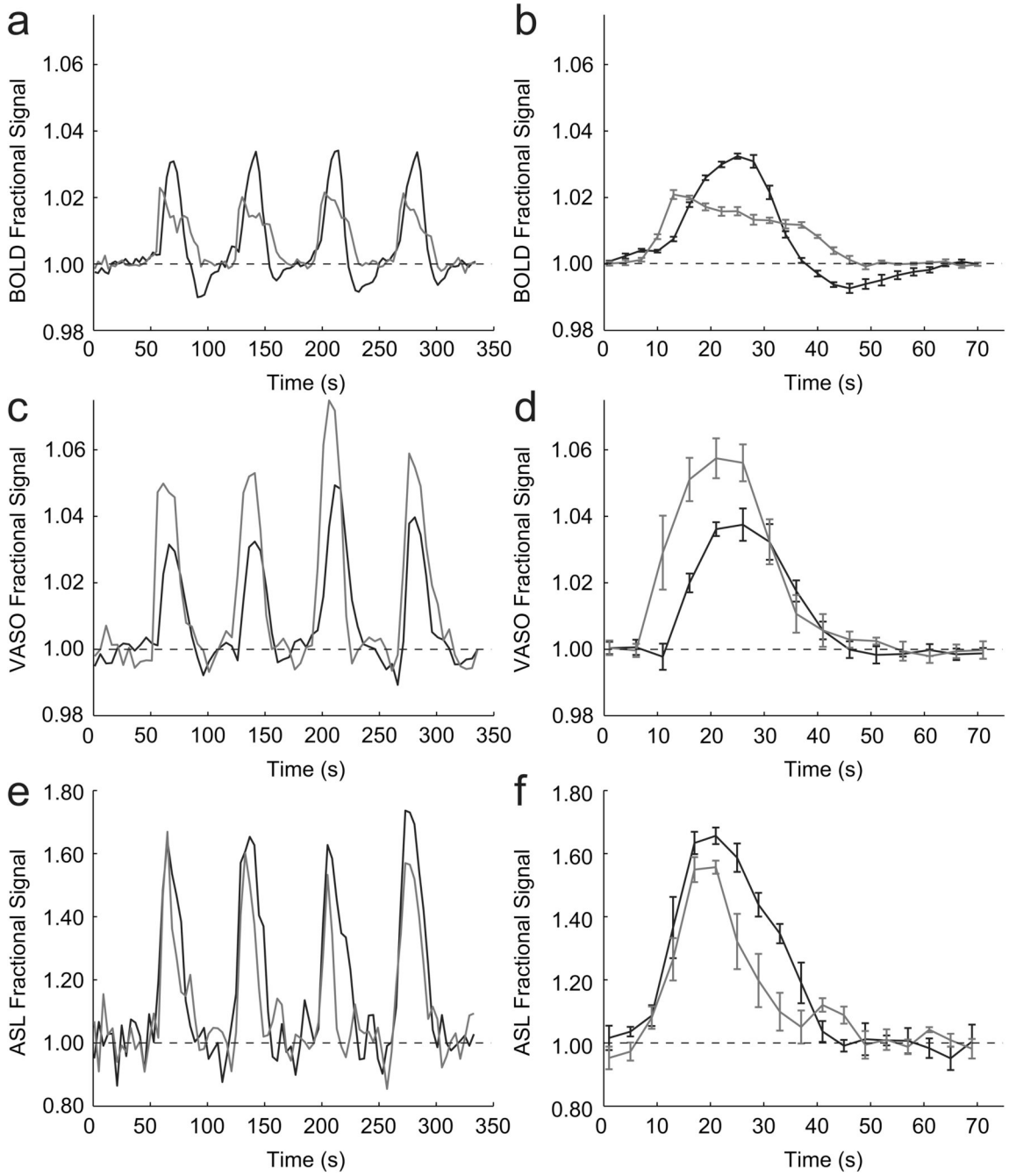

Figure 1.

Visual (black) and breath-hold (gray) time courses for voxels analyzed according to Method 1 voxel selection. On the left, the subject-averaged (n=9) time courses are shown for all four task periods; on the right, the block-averaged time courses are shown. (a,b) The BOLD time course shows a clear post-stimulus undershoot following visual stimulation, but not post-stimulus undershoot following breath-holding. In addition, the BOLD response during visual stimulation is larger than during breath-holding. (c,d) The CBVw time course (negative of the VASO signal change) shows no undershoot and a larger signal change during breath-hold than during visual stimulation. (e,f) The CBFw time course shows no post-stimulus undershoot in either task and comparable signal changes, within error, between task periods.

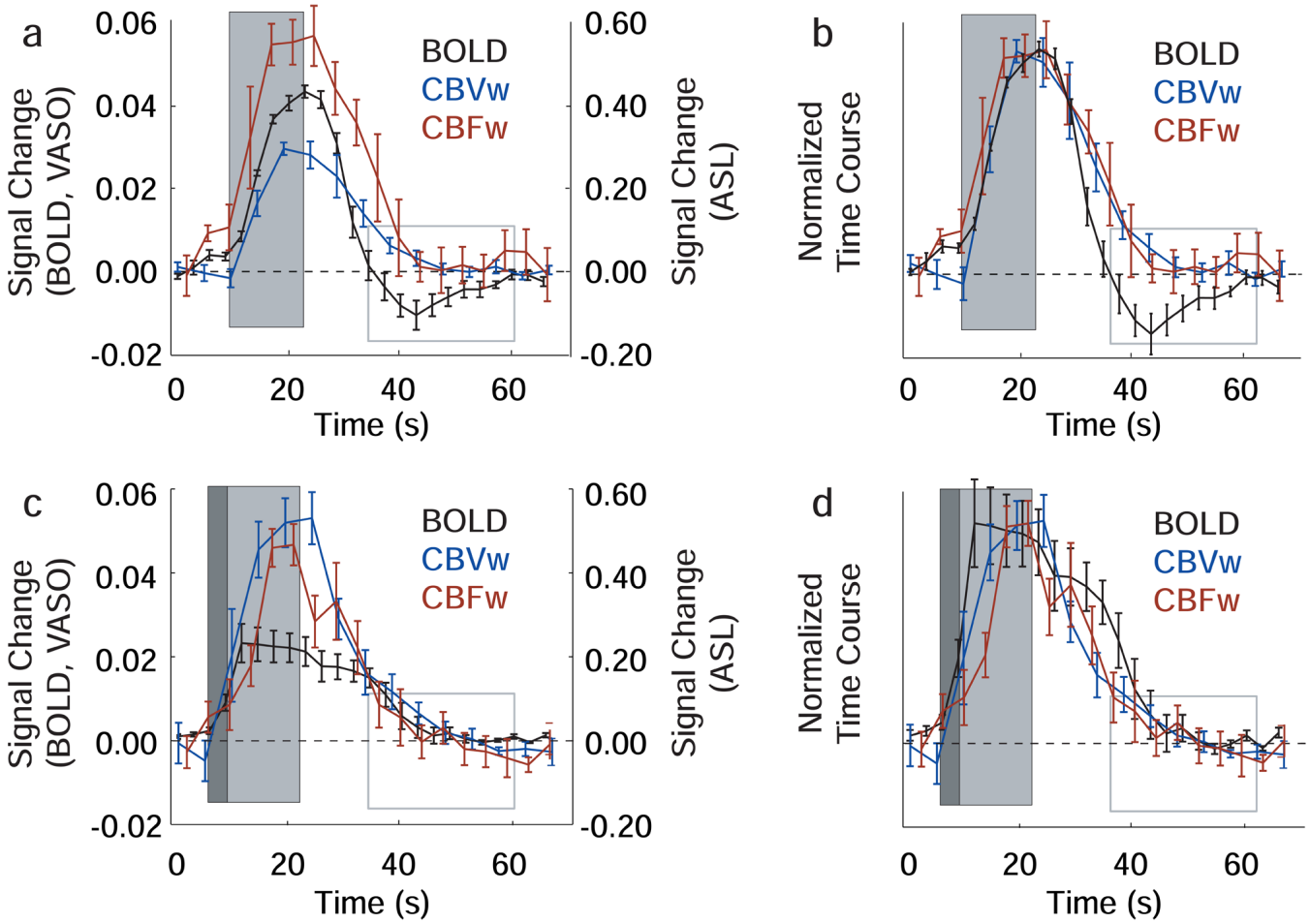

Figure 2.

BOLD, CBVw and CBFw time courses for voxels analyzed according to Method 2 voxel selection. Here, the four-block stimulus paradigm has been averaged to make direct comparison between modalities clearer. The dark gray box shows the duration of the exhale period, the light gray box shows the duration of the stimulus (visual or breath-hold) and the gray-lined box demarcates the location of the BOLD visual post-stimulus undershoot. (a) The visual time course shows a clear BOLD post-stimulus undershoot which persists during a period when the CBVw and CBFw signal have returned to baseline. (b) The visual time course normalized with respect to the maximum signal change. (c) The breath-hold time course shows that the BOLD, CBVw and CBFw responses return to baseline in the absence of any detectable undershoot. (d) The normalized breath-hold time courses.

J Cereb Blood Flow Metab. Author manuscript; available in PMC 2010 May 6.

Table 1

Physiological parameters (n = 9) measured before and after visual stimulation (above) and breath-hold (below).

	BOLD		**CBV_W**		**CBFw**	
Visual						
	Before	**After**	**Before**	**After**	**Before**	**After**
Heart Rate	66.4±8.3	66.8±8.2	68.3±9.3	67.2±9.7	65.2±7.9	65.1±7.9
S_{aO2}	97.4±1.5	97.4±1.5	97.7±1.3	97.7±1.3	97.7±0.9	97.7±0.9
$EtCO_2$	40.7±5.5	40.0±4.6	41.2±2.9	41.1±2.9	40.6±3.5	40.3±3.0
Breath-hold						
	Before	After	Before	After	Before	After
Heart Rate	65.7±10.8	66.0±9.3	65.2±8.3	64.3±7.9	65.9±7.8	66.1±8.7
S_{aO2}	97.6±1.1	97.6±1.2	96.9±1.7	97.2±1.3	97.8±1.4	98.0±1.3
$EtCO_2$	40.8±2.8	40.4±2.7	40.4±3.8	40.4±2.9	42.0±4.6	40.7±3.7

Values are mean over four task blocks; error represents standard deviation. During breath-hold, $EtCO_2$ was measured to be zero in all subjects. *Heart rate* is in beats/minute, S_{aO2} is arterial blood oxygenation in percent and $EtCO_2$ in mmHg.

Table 2

Individual signal changes (absolute % vs baseline) for BOLD, CBV-weighted (CBVw), and CBF-weighted (CBFw) hemodynamic responses.

	Visual stimulation			Breath-hold		
Subject	**BOLD**	**CBVw**	**CBFw**	**BOLD**	**CBVw**	**CBFw**
1	3.5±0.4	3.3±0.6	50±10	2.1±0.4	8.9±2.4	51±14
2	3.4±0.8	4.9±1.6	77±12	4.9±0.2	4.6±0.4	48±6
3	3.1±0.2	3.6±1.0	52±4	1.6±0.4	3.8±0.2	41±16
4	4.6±0.2	3.1±0.8	49±8	1.9±0.4	4.7±1.0	31±10
5	5.5±1.0	2.9±0.4	83±6	2.2±0.4	8.6±1.2	33±10
6	2.2±0.2	3.2±0.2	46±4	1.8±0.2	4.3±0.4	44±10
7	5.1±0.2	3.4±0.2	64±4	1.5±0.2	5.4±0.2	55±12
8	6.0±0.4	3.1±0.4	49±8	1.5±0.2	7.0±1.2	59±8
9	4.1±0.2	3.1±0.6	58±14	2.0±0.2	4.9±0.6	49±22
Mean	**4.2±1.2**	**3.4±0.6**	**59±13**	**2.2±1.1**	**5.8±1.9**	**46±9.4**

Method 2 was used for voxel selection to allow for comparison between imaging modalities. All values are mean ± standard deviation.

J Cereb Blood Flow Metab. Author manuscript; available in PMC 2010 May 6.

Table 3

Hemodynamic response times (s) for ultimate return to baseline (BOLD, CBVw and CBFw) and first touching (CBVw, CBFw) or crossing baseline (BOLD) following cessation of stimulus.

	Visual stimulation					
	Time (s) to return to baseline			**Time (s) to touch or cross baseline**		
Subject	**BOLD**	**CBVw**	**CBFw**	**BOLD**	**CBVw**	**CBFw**
1	39±8	26±6	18±8	17±8	22±4	18±8
2	29±4	17±10	16±8	18±8	17±10	12±6
3	32±4	20±6	16±6	9.0±4	17±6	16±6
4	33±8	24±6	17±4	20±8	24±6	17±4
5	24±6	13±6	20±6	8.0±4	13±6	14±2
6	28±2	26±12	26±8	13±6	22±6	26±8
7	38±2	16±2	23±4	16±8	16±2	12±6
8	36±4	14±2	20±4	12±6	14±2	20±4
9	38±6	26±6	22±10	15±6	22±2	22±10
Mean	**33±5**	**20±5**	**20±3**	**14±4**	**19±4**	**17±5**
	Breath-hold stimulation					
	Time (s) to return to baseline			Time (s) to touch or cross baseline		
Subject	BOLD	CBVw	CBFw	BOLD	CBVw	CBFw
1	21±6	21±10	18±14	21±6	21±10	10±2
2	28±12	22±6	19±4	24±10	22±6	17±6
3	29±6	31±6	20±8	29±6	29±6	20±8
4	30±8	13±10	14±2	30±8	8.0±2	14±2
5	19±6	20±4	14±6	17±4	16±6	14±6
6	25±8	30±8	23±8	22±8	30±8	23±8
7	28±8	19±4	18±12	20±2	19±4	18±12
8	9.0±4	15±6	16±8	9.0±4	15±6	16±8
9	19±8	19±6	19±4	19±8	19±6	19±4
Mean	**23±7**	**21±6**	**18±3**	**21±6**	**20±7**	**17±4**

Time to return to baseline with no further change (left) and time to touch or cross baseline after stimulus (right). All values are mean ± standard deviation over the four task repetitions. Method 2 was used for voxel selection to allow for comparison between imaging modalities. Baseline defined as mean signal intensity of all images acquired more than 5s before and/or 35s after any stimulus period.